ELSEVIER

Contents lists available at ScienceDirect

# Fish and Shellfish Immunology

journal homepage: www.elsevier.com/locate/fsi



Full length article

# Black carp RNF135 enhances RIG-I-mediated antiviral signaling by facilitating its oligomerization

Chushan Dai <sup>a,1</sup>, Yujia Miao <sup>a,1</sup>, Zhan'ao Li <sup>a</sup>, Yumian Liu <sup>a</sup>, Ji Liu <sup>a</sup>, Xiaoyu Liu <sup>a</sup>, Shasha Tan <sup>a</sup>, Hui Wu <sup>a</sup>, Jun Xiao <sup>a,b,\*</sup>, Jun Zou <sup>c</sup>, Hao Feng <sup>a,b,\*\*</sup>

- a State Key Laboratory of Developmental Biology of Freshwater Fish, College of Life Science, Hunan Normal University, Changsha, 410081, China
- <sup>b</sup> Institute of Interdisciplinary Studies, Hunan Normal University, Changsha, 410081, China
- <sup>c</sup> Key Laboratory of Exploration and Utilization of Aquatic Genetic Resources, Ministry of Education, Shanghai Ocean University, Shanghai, 201306, China

#### ARTICLE INFO

#### Keywords: RNF135 RIG-I IFN Oligomerization Black carp

#### ABSTRACT

RNF135, also known as RIPLET, plays a crucial role in facilitating RIG-I signaling in mammals. However, the function and regulatory mechanism of RNF135 in teleosts remain much to be elucidated. In this study, RNF135 homolog of black carp (bcRNF135) has been cloned and identified. The coding sequence (CDS) of bcRNF135 gene comprises 1221 nucleotides, encoding a protein of 407 amino acids. Immunoblotting (IB) and immunofluorescence (IF) assays identified that bcRNF135 is approximately 50 kDa and localized in the cytoplasm. qRT-PCR demonstrated that bcRNF135 mRNA levels were increased in host cells following SVCV infection and poly (I: C) stimulation. Co-expressed bcRNF135 obviously enhanced the induced transcription of IFN promoters by bcRIG-I in reporter assay, as well as improved bcRIG-I triggered antiviral response. Notably, bcRNF135 knockdown reduced the antiviral ability of host cells and increased virus replication. Co-immunoprecipitation (Co-IP) assays and IF assays confirmed that bcRNF135 interacted with bcRIG-I. Moreover, SDD-AGE revealed that bcRNF135 promotes the oligomerization of bcRIG-I, a process critical for RIG-I activation. Overall, our data conclude that bcRNF135 enhances bcRIG-I-mediated antiviral signaling by facilitating its ubiquitination and oligomerization, enriching our understanding of RIG-I regulation in teleost innate immunity.

#### 1. Introduction

The innate immune system plays a pivotal role in protecting vertebrates from the invasion of diverse pathogens [1]. This defense mechanism is reliant on pattern recognition receptors (PRRs), which are capable of identifying pathogen-associated molecular patterns (PAMPs) and initiating immune response [2]. One such PRR is retinoic acid-inducible gene-I (RIG-I), which belongs to the RIG-I-like receptors and recognizes cytosolic viral RNA, initiating downstream signaling [3]. Upon infection with an RNA virus, RIG-I becomes activated and binds to the mitochondrial antiviral-signaling protein (MAVS), which in turn transmits signals to TBK1 and IKKE, activating IRF3 and IRF7, thereby inducing the expression of type I interferon (IFN) [4,5].

To maintain immune homeostasis, the activity of RIG-I is strictly

regulated by various mechanisms to avoid detrimental inflammatory responses [6,7]. Ubiquitination, a widespread post-translational modification (PTM), is critical for regulating functional proteins [8]. The ubiquitin (Ub) chains conjugate to target proteins at specific lysine residues (K6/K11/K27/K29/K33/K48/K63) or the amino-terminal methionine, leading to distinct protein functions [9,10]. For instance, TRIM25 mediates the K63-linked ubiquitination of RIG-I, promoting RIG-I-mediated interferon production in mammalian cells [11]. Additionally, USP4 facilitates antiviral response by inhibiting the K48-linked ubiquitination of RIG-I [12]. Conversely, TRIM40 limits antiviral immune responses by promoting the K27- and K48-linked ubiquitination of RIG-I [13]. In teleost, zebrafish TRIM25 promotes the K63-linked ubiquitination of 2CARD and RD regions of RIG-I to positively regulate its antiviral activity [14].

<sup>\*</sup> Corresponding author. State Key Laboratory of Developmental Biology of Freshwater Fish, College of Life Science, Hunan Normal University, Changsha, 410081, China.

<sup>\*\*</sup> Corresponding author. State Key Laboratory of Developmental Biology of Freshwater Fish, College of Life Science, Hunan Normal University, Changsha, 410081, China.

E-mail addresses: xiaojun2018@hunnu.edu.cn (J. Xiao), fenghao@hunnu.edu.cn (H. Feng).

 $<sup>^{1}\,</sup>$  These authors contributed equally to this paper.

Ring finger protein 135 (RNF135) functions as E3 ubiquitin ligase and is essential for ubiquitination. It is a member of the RNF protein family and comprises an N-terminal RING finger domain, C-terminal SPRY, and PRY motifs. In mammals, RNF135 was first reported to facilitate the activation of RIG-I in 2009 [15]. Subsequent studies have provided evidence indicating that RNF135 positively regulates K63-linked ubiquitination of the RIG-I in human antiviral innate immunity [16]. Similarly, the knockout of endogenous RNF135 in mice inhibited RIG-I activation in response to RNA virus infection and was defective in the secretion of IFN and other cytokines during infection with several RNA viruses [17]. However, research on the function of RNF135 in fish is limited.

Our previous research indicates that black carp RIG-I (bcRIG-I) significantly induces IFN production and exhibits strong antiviral activity. Nevertheless, the regulatory mechanism underlying its antiviral activity remains largely unknown [18]. In this study, we successfully cloned and identified the function of black carp RNF135 (bcRNF135). Our results discovered that bcRNF135 serves as a positive regulator of bcRIG-I in the host's antiviral innate immune responses. In mechanism, bcRNF135 interacts with bcRIG-I, facilitating its ubiquitination and oligomerization, thereby augmenting its antiviral activity. These results provide novel insights into the regulatory mechanism of RIG-I by RNF135 in teleosts.

#### 2. Materials and methods

#### 2.1. Cells and plasmids

Epithelioma papulosum cyprini (EPC), *Mylopharyngodon piceus* kidney (MPK), *Mylopharyngodon piceus* fin (MPF), human embryonic kidney 293T (HEK293T) and Hela cells were cultured in Dulbecco's modified Eagle's medium (DMEM) supplemented with 10 % FBS, 2 mML-glutamine, 100 U/ml penicillin and 100 mg/ml streptomycin in 5 % a CO2 incubator. EPC, MPK and MPF cells were kept at 28  $^{\circ}$ C, while HEK293T and Hela cells were cultured at 37  $^{\circ}$ C.

The plasmids pcDNA5/FRT/TO (Invitrogen, USA), Luci-bcIFNa (for black carp IFNa promoter activity analysis), Luci-eIFN (for EPC IFN promoter activity analysis), Luci-DrIFN $\phi$ 1 (for zebrafish IFN $\phi$ 1 promoter activity analysis), Luci-DrIFN $\phi$ 3 (for zebrafish IFN $\phi$ 3 promoter activity analysis), pRL-TK and pcDNA5/FRT/TO-HA-Ub were kept in our lab. The shRNA vector for knocking down bcRNF135 was constructed by inserting the shRNAs into PLKO.1, which was designed by the protocol on the website (http://rnaidesigner.thermofisher.com/rnaiexpress). All the primer sequences were referenced in Table 1.

### 2.2. Virus production and antiviral assay

Spring viremia of carp virus (SVCV/strain: SVCV741) was amplified in EPC cells using 2 % FBS at 28 °C. Virus titers were determined by plaque assay as previously described. For the antiviral assay, EPC cells seeded in 24-well plates were transfected with the indicated plasmids. At 24 h post-transfection, cells were infected with SVCV. After 24h of infection, the supernatant was collected and frozen at  $-80^{\circ}$ Cfor subsequent detection. Virus titration was performed using 10-fold dilutions of the corresponding cell supernatant added to EPC cells in 24-well plates. After incubation for 2 h at 28 °C, the supernatant was removed and replaced with fresh DMEM containing 2 % FBS and 0.75 % methylcellulose (Sangon, China). When cells exhibited obvious CPE, the viral spots in each well were counted using crystal violet staining.

### 2.3. Poly (I:C) and SVCV treatments

MPK and MPF cells were seeded in a 6-well plate (1  $\times$  10 $^6$  cells/well) 24 h before treatment. Poly (I:C) (Sigma, USA) was used for synthetic dsRNA stimulation, which was heated to 55  $^{\circ}$ C (in PBS) for 5 min and cooled to room temperature. MPK cells were treated with fresh media

Table 1
Primers used in the study.

Primer	Sequence (5'-3')	Application
q-bcRNF135-	CACAACACGCTGGGAGAA	For qRT-PCR
F		
q-bcRNF135-	CTGGGGAGAGAAGGAAAG	
R		
q-SVCV-M-F	CGACCGCCCAGTATTGATGGATAC	
q-SVCV-M-R	ACAAGGCCGACCCGTCAACAGAG	
q-SVCV-P-F	AACAGGTATCGACTATGGAAGAGC	
q-SVCV-P-R	GATTCCTCTTCCCAATTGACTGTC	
q-SVCV-G-F	ATGAGGGATAATATCGGCTTG	
q-SVCV-G-R	TGCATTGTCTCCACCTGGCT	
q-bcIFNa-F	AAGGTGGAGGACCAGGTGAAGTTT	
q-bcIFNa-R	GACTCCTTATGTGATGGCTTGTGG	
q-bcIFNb-F	GACCACGTTTCCATATCTTT	
q-bcIFNb-R	CATTTTTCTTCATCCCACT	
q-bcβ-actin-F	TGGGCACCGCTGCTTCCT	
q-bcβ-actin-R	TGTCCGTCAGGCAGCTCAT	
q-bcViperin- F	CCAAAGAGCAGAAAGAGGGACC	
q-bcViperin- R	TCAATAGGCAAGACGAACGAGG	
q-bcPKR-F	GAGCGGACTAAAAGGACAGG	
q-bcPKR-R	AAAATATATGAGACCCAGGG	
q-bcMX1-F	TGGAGGAACCTGCCTTAAATAC	
q-bcMX1-R	GTCTTTGCTGTTGTCAGAAGATTAG	
18T- bcRNF135- F	ATGATGTCGGCATTATATG	For CDS cloning
18T- bcRNF135- R	ATGTCTAGGAAAGGTTAAG	
N-	ACTGACGGTACCGCCACCAT	For expression
bcRNF135-	GATGTCGGCATTATATG	vector construction
F		
N-	ACTGACCTCGAGtcaAtgTCTA	
bcRNF135- R	GGAAAGG	
C-bcRNF135-	ACTGACGGTACCGCCACCAT	
F	GATGTCGGCATTATATG	
C-bcRNF135-	ACTGACCTCGAGAtgTCTAGG	
R	AAAGGTTAAGGC	
ShRNF135-1-	AATTCAAAAAGGAGCAGATTATGGCAGAA	shRNA
F	ACCTCGAGGTTTCTGCCATAATCTGCTCC	
ShRNF135-1-	GGAGCAGATTATGGCAGAAACCTCGAGGT	
R	TTCTGCCATAATCTGCTCCTTTTTGAATT	
ShRNF135-2-	CCGGGCAAAGTTTGTTGAGCTTTCCCTCG	
F	AGGGAAAGCTCAACAAACTTTGCTTTTTG	
ShRNF135-2-	CAAAAAGCAAAGTTTGTTGAGCTTTCCCT	
R	CGAGGGAAAGCTCAACAAACTTTGCCCGG	

containing poly (I:C) at different concentrations (5  $\mu g/ml$  or 25  $\mu g/ml)$  and harvested at different time points post-treatment. For SVCV infection, MPK and MPF cells in 6-well plates (1  $\times$  10 $^6$  cells/well) were treated with SVCV at different MOIs and harvested at different time points post-infection.

#### 2.4. RNA extraction and Quantitative real-time PCR (qRT-PCR)

Total RNAs from treated cells in 6-well plates were extracted using the RNA rapid extraction kit (Magen, China). First-strand cDNA synthesis was carried out using reverse transcriptase (Takara, Japan). qRT-PCR was performed to detect relative mRNA levels using the Applied Biosystems QuantStudio 5 Real-Time PCR Systems (Thermo Fisher, USA). The qRT-PCR programs were as follows: 1 cycle of 95 °C/10 min, 40 cycles of 95 °C/15 s, 60 °C/1 min. The relative changes of target genes were calculated by comparison with control groups using the 2  $^{-\Delta\Delta CT}$  methods.  $\beta$ -actin was used as the internal control.

#### 2.5. Dual-luciferase reporter assay

EPC cells were cultured in 24-well plates and transfected with the

described plasmids together with pRL-TK and different IFN promoters. The total amount of plasmids was balanced with the empty vectors. After 24 h post-transfection, the cells were lysed using passive lysis buffer (PLB) for 15 min on ice. Then the supernatant was used to measure the activities of firefly luciferase and renilla luciferase by dual-luciferase reporter assay system (Promega, USA).

#### 2.6. Immunofluorescence microscopy

HeLa cells were transfected with the indicated plasmids using LipoMax (Sudgen, China) for 24 h. Subsequently, the cells were fixed with 4 % paraformaldehyde for 15 min and permeabilized with Triton X-100 (0.2 % in PBS) for 15 min. The cells were then blocked with 10 % goat serum (solarbio SL038) for 1 h and stained using the anti-Flag antibody (Abmart, M20008) or anti-HA antibody (Abmart, M20003) for 2 h. After being washed six times with PBS, the corresponding secondary antibodies, Alexa 594 (Thermo, 35511) and Alexa 488 (Thermo, 35553), were probed at the ratio of 1:1000. DAPI (Sigma, USA) was used for nuclear staining. Finally, the cells were scanned under a confocal microscope (Olympus).

#### 2.7. Western blotting

HEK293T cells and EPC cells in 6-well plates were transfected with the plasmids described in the figures. For sample preparation, the cells were collected after 24 h post-transfection and mixed with  $5 \times SDS$  loading buffer, boiled for approximately 45 min. Subsequently, the samples were separated by SDS-polyacrylamide gels at appropriate concentrations. The proteins transferred to polyvinylidene fluoride (PVDF) membranes (Millipore, USA) were blocked for 1 h at room temperature in skim milk and incubated with the primary antibodies at appropriate dilutions overnight at 4  $^{\circ}C$ . After washing three times with TBST and once with TBS, the membranes were stained with the secondary antibodies for 1 h. Lastly, the target proteins were detected by BCIP/NBT Alkaline Phosphatase Color Development Kit (Sigma, USA).

#### 2.8. Co-immunoprecipitation (Co-IP)

HEK293T cells seeded in 10 cm² dishes were transfected with the plasmids shown in the figures and harvested for Co-IP assay after 48 h. Sample preparation involved washing the cells with ice-cold PBS and lysing them with 1 % NP-40 lysis buffer containing protease inhibitor cocktails. The cell debris was removed by centrifugation at 12,000×g for 10 min at 4 °C, and the supernatants were transferred to new tubes for incubation with protein A/G agarose beads at 4 °C for 1 h. After centrifugation at 5000 rpm for 2 min at 4 °C, the supernatants were collected to incubate with Anti-Flag-conjugated (or anti-HA-conjugated) agarose beads at 4 °C overnight with constant agitation. The samples were washed with 1 % NP-40 buffer for 4 times and then boiled for western blotting as above.

#### 2.9. Knockdown assay

Using a shRNA library from Sigma, the shRNA oligos were created based on the nucleotide sequence of bcRNF135. As instructed by the protocol, primers were added to ddH $_2\text{O}$  and diluted to 20  $\mu\text{M}$ . To the PCR tubes, according to the annealing system, 5  $\mu\text{l}$  of each oligonucleotide, 25  $\mu\text{l}$  of 10  $\times$  NEB buffer, and 5  $\mu\text{l}$  of ddH $_2\text{O}$  were added. The tubes were then annealed for 5 min in a 95 °C water bath before being cooled to room temperature. The PLKO.1 vector (1  $\mu\text{g}$ ) was double-digested with restriction endonucleases EcoR I and AgeI. Subsequently, the primers were ligated to the vectors, purified, and subjected to sequencing.

#### 2.10. Semi-denaturing detergent agarose gel electrophoresis (SDD-AGE)

Plasmids depicted in the figures were used to transfect HEK293T cells in 100 mm dishes, and the cells were harvested 48 h after transfection. Then the cells were treated with 1 % NP-40 lysis buffer and centrifuged. The supernatant was collected and mixed with 5  $\times$  loading buffer. Samples were then separated using a horizontal 1.5 % agarose gel, prepared with 1  $\times$  TBE and 0.1 % SDS, at a constant 100V for 80 min at 4  $^{\circ}$ C [19]. Following gel electrophoresis, the proteins were transferred to a PVDF membrane, incubated with primary and secondary antibodies, and visualized by NBT/BCIP, as described above.

#### 2.11. Statistics analysis

The data of dual-luciferase reporter assay, qRT-PCR, and viral titration were obtained from the average values of three independent experiments. Each experiment was repeated at least three times. The student's t-test was applied to suggest the statistical significance between the groups. Asterisk \* represents p < 0.05, which means statistically significant; \*\* stands for p < 0.01 which means the high significance of the statistic.

#### 3. Results

#### 3.1. Molecular cloning and sequence analysis of bcRNF135

To investigate the role of RNF135 in the innate immunity of black carp, the coding sequence (CDS) of bcRNF135 (GenBank: PP974314) was cloned and identified from MPK cells. The CDS comprises 1221 nucleotides and encodes a protein of 407 amino acids. To assess the conservation of RNF135 across vertebrates, we aligned the amino acid sequences of RNF135 proteins from black carp (Mylopharyngodon piceus), zebrafish (Danio rerio), mice (Mus musculus) and human (Homo sapiens) (Fig. 1A). Structure analysis represented that bcRNF135 harbors an N-terminal RING domain and a C-terminal SPRY domain (Fig. 1B). Utilizing phylogenetic analysis, we constructed a evolutionary tree comparing the amino acid sequences of RNF135 from various species, including birds, reptiles, amphibians, mammals and fish. The result revealed that bcRNF135 shared the highest similarity (96.8 %) with Megalobrama amblycephala (Fig. 1C). Further analysis of the black carp genome revealed that the bcRNF135 gene is situated on chromosome 6 and is composed of four exons (Fig. 1D).

#### 3.2. The mRNA expression of bcRNF135 in response to different stimuli

To investigate the modulation of bcRNF135 mRNA expression in response to various stimuli, MPK and MPF cells were subjected to diverse stimulation. qRT-PCR was employed to detect the bcRNF135 mRNA levels. In SVCV-infected MPK cells, bcRNF135 mRNA levels in the MOI 0.1 group and in the MOI 0.01 group peaked at 48 h postinfection (hpi), respectively (Fig. 2A). Treatment of MPK cells with poly (I:C) induced a significant upregulation of bcRNF135 mRNA, which was higher than in the control (Fig. 2B). In addition, SVCV-infected MPF cells exhibited a modest increase in bcRNF135 mRNA levels across all groups, except at the 8-h time point in the MOI 0.01 group. The highest bcRNF135 mRNA levels were observed at 48 hpi in the 0.01 and 0.1 MOI groups (Fig. 2C). Furthermore, when MPF cells were stimulated by poly (I:C), the bcRNF135 mRNA level in 25 µg/ml group at 48 h was approximately 11.5-fold of the control (Fig. 2D). The results above indicated that bcRNF135 may participate in the innate immune response activated by RNA viruses.

#### 3.3. Protein expression and subcellular distribution of bcRNF135

To further reveal the function of bcRNF135, we employed western blotting to examine its protein expression. Plasmids expressing

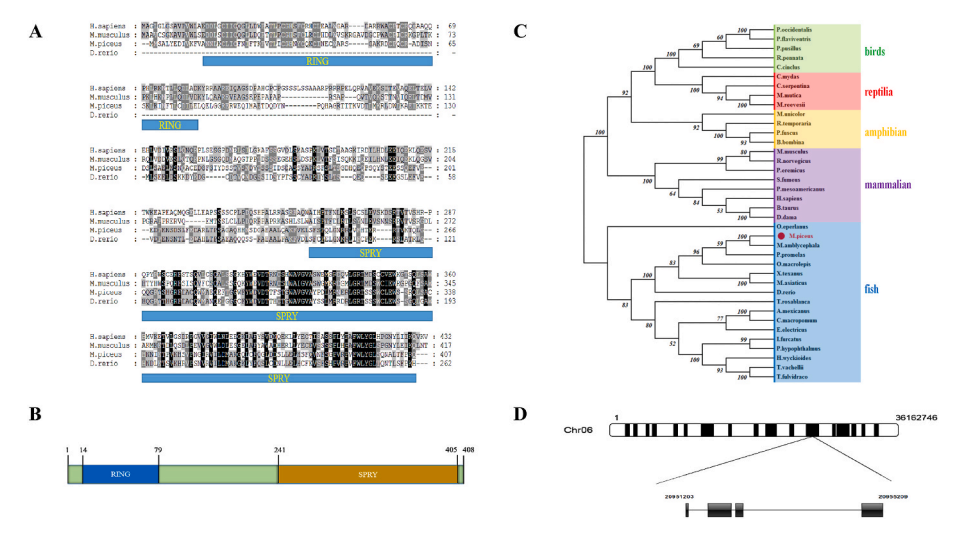


Fig. 1. Sequence analysis and evolution of bcRNF135

(A) The amino acid sequence analysis of bcRNF135 with *H. sapiens* (NP\_115698.3), *M. musculus* (NP\_082295.1), and *Danio rerio* (XP\_021329759.1) were aligned by MEGA-X and GENEDOC. (B) The conserved protein domains of bcRNF135 were constructed by IBS 2.0 (https://ibs.renlab.org/#/server). (C) The phylogenetic tree was built by MEGA-X. Genebank accession numbers of species are shown in Table S1. (D) The chromosome analysis of bcRNF135 was constructed by the online tool IBS (http://ibs.biocuckoo.org/online.php#).

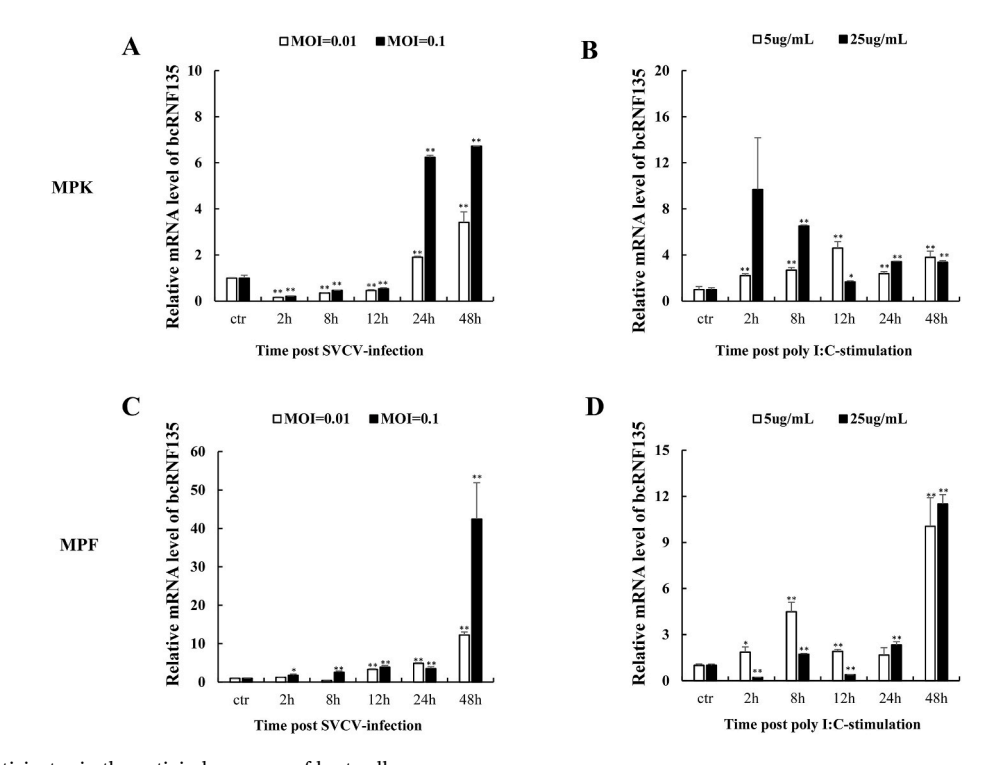


Fig. 2. bcRNF135 participates in the antiviral response of host cells (A-D): MPK (A&B) or MPF (C&D) cells seeded in 6-well plates ( $1 \times 10^6$  cells/well) were infected with SVCV or treated with poly (I:C). The cells were harvested at different time points and applied to qRT-PCR to detect the mRNA levels of bcRNF135. The asterisk (\* or \*\*) indicates the significant difference compared to the 0 h group. \*p < 0.05, \*\*p < 0.01.

bcRNF135 were transfected into HEK293T and EPC cells individually, followed by western blot analysis. As shown in Fig. 3A and B, bcRNF135 was well expressed in both HEK293T and EPC cells, with a specific band corresponding to approximately 50 kDa. To investigate the subcellular distribution of bcRNF135, we transfected the plasmids into HeLa cells and performed immunofluorescence assays. The result revealed that bcRNF135 predominantly localized to the cytoplasm (Fig. 3C). In addition, the protein three-dimensional structure of bcRNF135 and human RNF135 (hRNF135) was constructed by the SWISS MODEL

(https://swissmodel.expasy.org/). As shown in Fig. 3D, bcRNF135 and hRNF135 had a comparable structure, suggesting that they might have similar functions (Fig. 3D).

## 3.4. bcRNF135 enhanced bcRIG-I-mediated IFN promoter transcription

Previous studies have demonstrated that RNF135 serves as a positive regulator of RIG-I [16,20,21]. To examine the function of bcRNF135 in IFN signaling pathway of black carp, the dual-luciferase reporter assays

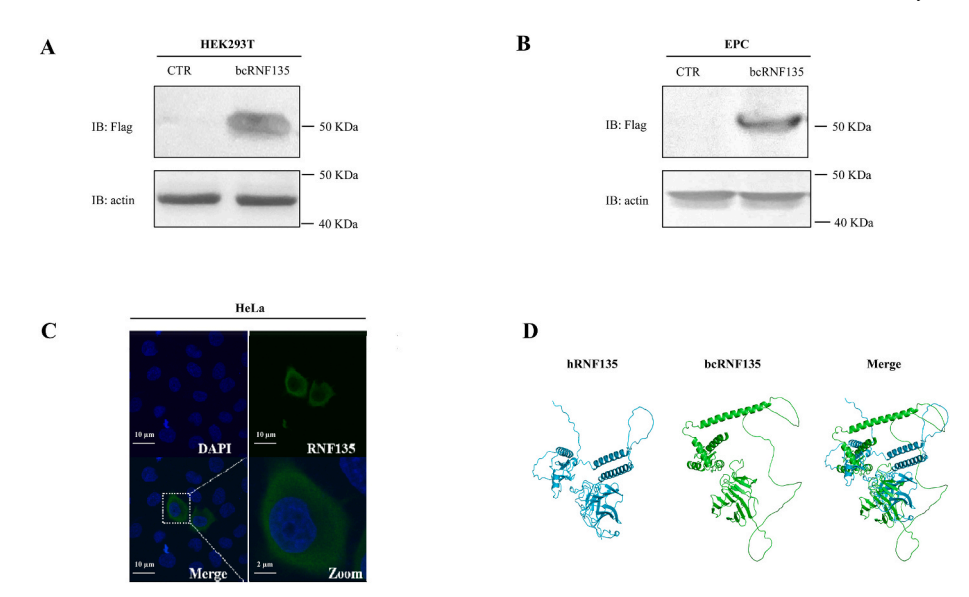


Fig. 3. The protein expression and subcellular distribution of bcRNF135 (A&B) HEK293T cells (A) and EPC cells (B) were seeded in 6-well plates ( $2\times10^6$  cells/well). The cells were transfected with empty vector or the plasmid expressing bcRNF135 (3  $\mu$ g/well), individually. At 48 hpt, the cells were collected for the western blotting. (C): Hela cells in 24-well plate ( $5\times10^4$  cells/well) were transfected with bcRNF135 (400ng/well) and subjected to the immunofluorescence assay at 24 hpt. The localization of bcRNF135 is shown in green, and the nucleus is shown in blue. (D) The three-dimensional structure of RNF135 protein was predicted by SWISS-MODEL. CTR: pcDNA5/FRT/TO; bcRNF135: pcDNA5/FRT/TO-Flag-bcRNF135.

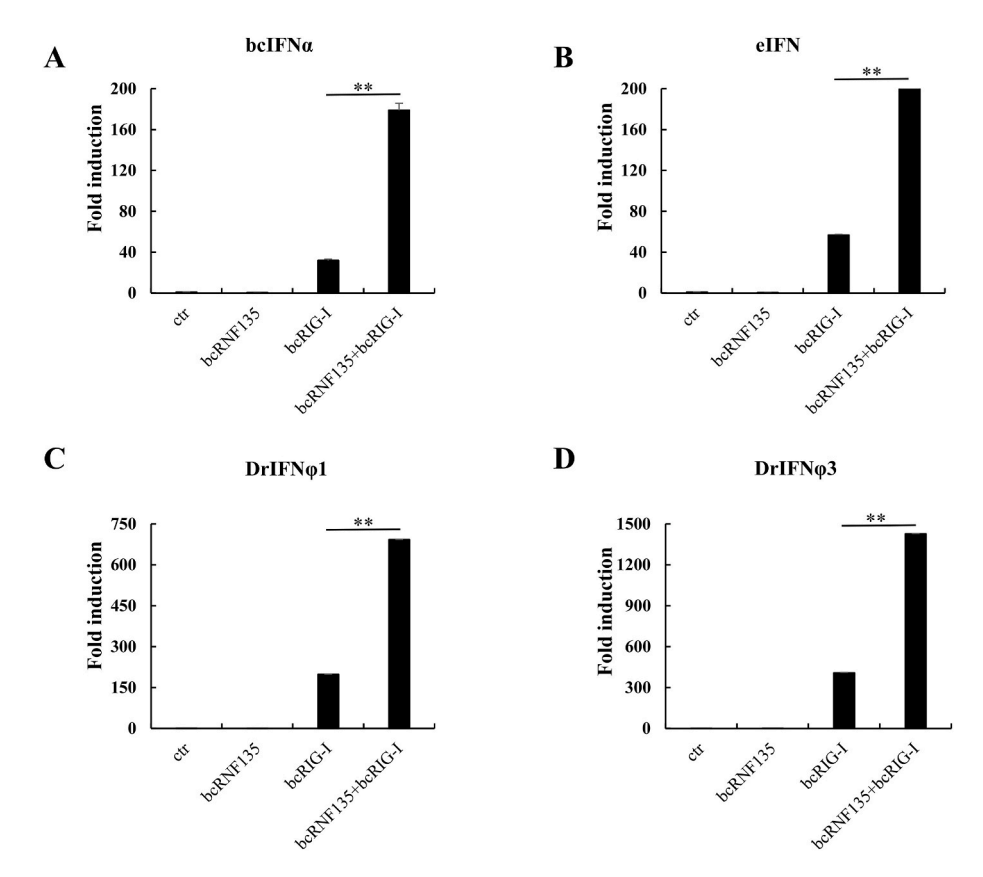


Fig. 4. bcRNF135 enhances bcRIG-I-mediated interferon promoter transcription (A-D): EPC cells in 24-well plates ( $4 \times 10^5$  cells/well) were co-transfected with pRL-TK (25 ng) and the empty vector (500 ng)/bcRNF135 (250 ng)/bcRIG-I (250 ng)/bcRNF135 (250 ng). The qualities of the transfection plasmids were balanced by the empty vector. The promoter induction fold of bcIFNa (A), eIFN (B), DrIFN $\phi$ 1 (C), and DrIFN $\phi$ 3 (D) were detected by the dual-luciferase reporter assay. The data comes from three independent replicates. CTR: pcDNA5/FRT/TO; bcRNF135: pcDNA5/FRT/TO-bcRIG-I-Flag. \*p < 0.05, \*\*p < 0.01.

were performed. The results revealed that bcRIG-I, when expressed individually, significantly activates the four promoters of bcIFN (Fig. 4A), eIFN (Fig. 4B), DrIFN $\phi$ 1 (Fig. 4C), and DrIFN $\phi$ 3 (Fig. 4D). The activation of these promoters is further enhanced when bcRNF135 is co-expressed with bcRIG-I. These findings suggest that bcRNF135 significantly amplifies bcRIG-I's ability to stimulate IFN promoter activity.

#### 3.5. bcRNF135 facilitated bcRIG-I-mediated antiviral activities

We further explored the effect of bcRNF135 on bcRIG-I-mediated antiviral activity. EPC cells were transfected with bcRNF135 and/or bcRIG-I and then infected with SVCV. Crystalline violet staining revealed that the cytopathic effect was significantly reduced in cells transfected with both bcRNF135 and bcRIG-I, compared to other groups (Fig. 5A). Simultaneously, the viral titers in the supernatant of cells cotransfected with bcRNF135 and bcRIG-I were significantly lower than those in the supernatant of cells transfected with bcRNF135 or bcRIG-I alone (Fig. 5B). Meanwhile, qRT-PCR analysis indicated that the transcriptions of virus proteins (SVCV-M, N, P, and G) were attenuated in the cells co-transfected with bcRIG-I and bcRNF135, compared to cells transfected with bcRIG-I only (Fig. 5C-F). To sum up, these results demonstrated that bcRNF135 enhances the antiviral activities mediated by bcRIG-I.

# 3.6. The knockdown of bcRNF135 weakened the antiviral ability of MPK cells

To validate the importance of bcRNF135 in RIG-I-mediated antiviral signaling, we designed shRNAs to specifically reduce bcRNF135 mRNA levels. In Fig. 6A, the western blot analysis was performed to assess the knockdown efficiency of different shRNAs targeting bcRNF135 in HEK293T cells. The results indicate that sh-2 led to the most substantial reduction in bcRNF135 protein levels, while sh-1 showed a moderate knockdown efficiency. The scramble control exhibited no reduction in bcRNF135 expression. These findings suggest that sh-2 is the most

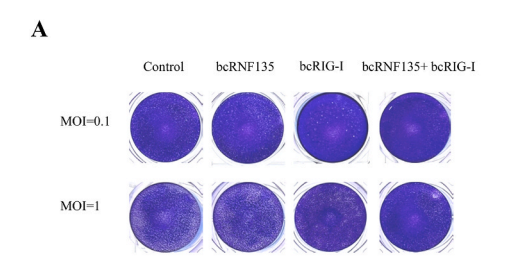
effective in knocking down bcRNF135 in HEK293T cells. Subsequently, MPK cells (derived from Mylopharyngodon piceus kidney) were transfected with scramble or sh-2. The knockdown efficiency of endogenous bcRNF135 was assessed using qRT-PCR. The results showed that the knockdown reduced the mRNA expression of bcRNF135 to approximately 60 % compared to the control. This confirms the effective knockdown of bcRNF135 in its native host cells (Fig. 6B). Besides, the transcripts of bcPKR, bcIFNa, and bcViperin were decreased in bcRNF135-knockdown cells infected with SVCV (MOI = 0.1), comparing to the control group (Fig. 6C-E). Furthermore, qRT-PCR data showed that the knockdown of bcRNF135 led to increased transcription of SVCV viral proteins (M, N, P, and G) (Fig. 6F-I). Consistent with these observations, the virus tite was significantly higher in bcRNF135knockdown MPK cells upon SVCV infection (MOI = 0.1) than in the control group (Fig. 6J). These findings indicate that the knockdown of bcRNF135 impairs the antiviral ability of MPK cells.

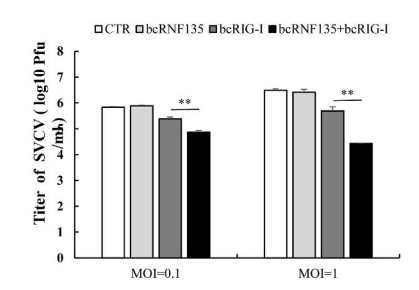
#### 3.7. The interaction between bcRNF135 and bcRIG-I

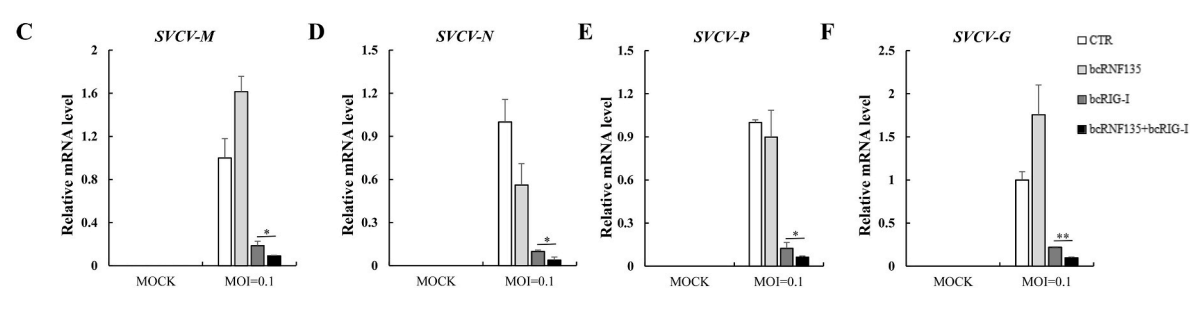
To reveal the regulation mechanism underlying bcRNF135 modulates bcRIG-I signaling, we investigated the interaction between these two proteins. Immunofluorescence microscopy revealed co-localization of bcRNF135 and bcRIG-I in the cytoplasm, suggesting their potential interaction (Fig. 7A). To validate this, co-IP assays were performed using HEK293T cells transfected with both bcRNF135-Flag and bcRIG-I-HA. The results showed that bcRNF135-Flag could be precipitated by bcRIG-I-HA, with a specific band at approximately 50 kDa observed (Fig. 7B). Simultaneously, when bcRNF135-Flag was used as the decoy protein, a distinct band at around 100 kDa indicated the presence of bcRIG-I-HA in the precipitated complex (Fig. 7C). These data collectively suggest that bcRNF135 interacts with bcRIG-I.

# 3.8. bcRNF135 promoted the ubiquitination and oligomerization of bcRIG-I

Given that the activation of RIG-I requires ubiquitination and the







В

Fig. 5. bcRNF135 facilitates bcRIG-I-mediated antiviral activities (A&B) EPC cells were seeded in 24-well plates ( $4 \times 10^5$  cells/well). The plasmids indicated in the figure were transfected into EPC cells. At 24 hpt, the cells were infected with SVCV at different MOI (MOI = 0.1, MOI = 1). Then cells were used for crystal violet staining (A) and the supernatant was collected for the detection of virus titer(B). (C–F) EPC cells in 6-well plates ( $2 \times 10^6$  cells/well) were transfected with empty vector/bcRNF135 (750 ng)/bcRIG-I (750 ng)/bcRNF135 (750 ng) & bcRIG-I (750 ng). The total amount of the plasmids was balanced by the empty vector. At 24 hpt, cells were infected with or without SVCV (MOI = 0.1). The cells were harvested after 24h then the relative mRNA level of SVCV-M (C), SVCV-N (D), SVCV-P (E), and SVCV-G (F) was tested by the qRT-PCR.

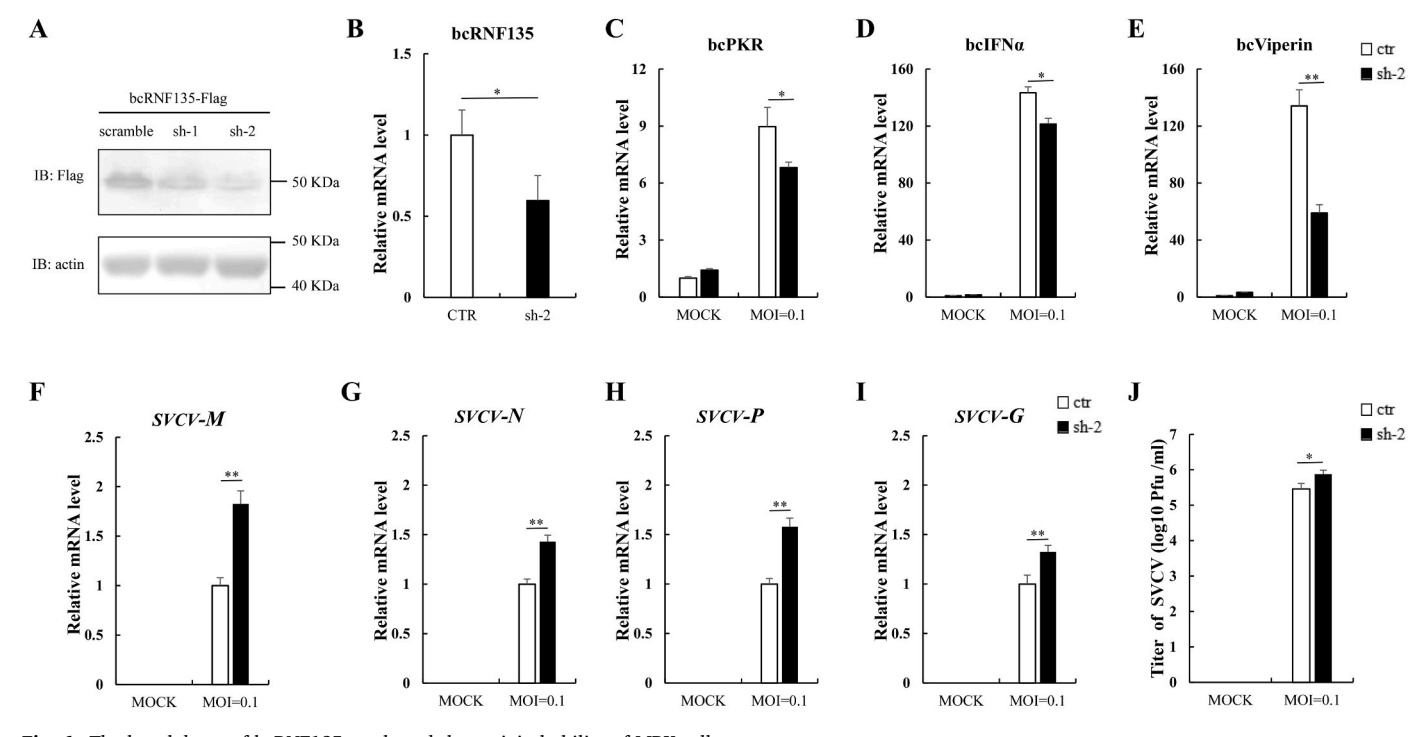


Fig. 6. The knockdown of bcRNF135 weakened the antiviral ability of MPK cells (A) HEK293T cells in the 6-well plate ( $2 \times 10^6$  cells/well) were transfected with pcDNA5/FRT/TO-Flag-bcRNF135 (750 ng) and scramble (750 ng)/shbcRNF135-1 (750 ng)/shbcRNF135-2 (750 ng). The knockdown efficiency of bcRNF135 was tested by Western blotting. (B) MPK cells seeded in 6-well plates ( $1 \times 10^6$  cells/well) were co-transfected with pcDNA5/FRT/TO-Flag-bcRNF135 and Scramble/shbcRNF135-2. After reverse transcription, the relative mRNA level of bcRNF135 was detected by qRT-PCR. (C–J) MPK cells seeded in 6-well plates ( $1 \times 10^6$  cells/well) were transfected with scramble (750 ng) or shbcRNF135-2 (750 ng), and infected with SVCV at indicated MOI (MOCK: the uninfected group serves as the control group). The transcription levels of IFN signaling pathway related factors bcPKR (C), bcIFNa (D) and bcViperin (E) in MPK cells were detected by qRT-PCR at 24 hpt. The relative mRNA levels of SVCV protein SVCV-M (F), SVCV-N (G), SVCV-P (H), and SVCV-G (I) were also detected by qRT-PCR; The supernatant was used for the detection of virus titer (J). Each data repeated at least three times. \*p < 0.05, \*\*p < 0.01.

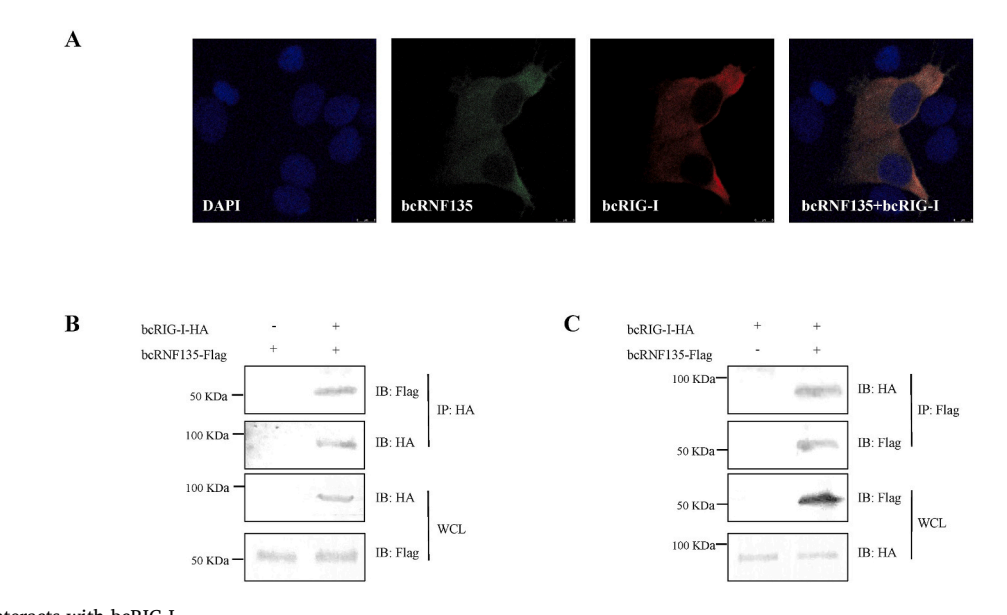


Fig. 7. bcRNF135 interacts with bcRIG-I (A) Hela cells in 24 well-plates ( $5 \times 10^4$  cells/well) were transfected with bcRNF135 (200 ng) and bcRIG-I (200 ng). The cells were collected for immunofluorescence assay at 24 h post-transfection. bcRNF135: pcDNA5/FRT/TO-Flag-bcRNF135. bcRIG-I: pcDNA5-FRT/TO-bcRIG-I-HA. (B–C): HEK293T cells in 100 mm plates were co-transfected with pcDNA5-FRT/TO-bcRIG-I-HA ( $7.5 \mu$ g) and pcDNA5/FRT/TO-bcRNF135-Flag ( $7.5 \mu$ g). At 48 hpt, the cells were incubated with anti-HA-conjugated agarose beads (B) or anti-Flag-conjugated agarose beads (C), respectively. IP: immunoprecipitation. WCL: whole cell lysate.

formation of oligomers. Further insights into how bcRNF135 enhances bcRIG-mediated antiviral responses were sought through the use of the Co-IP assay and the SDD-AGE assay. The Co-IP assay showed that

ubiquitination of bcRIG-I was significantly promoted by bcRNF135, comparing to the group transfected with bcRIG-I alone (Fig. 8A). This result indicates that bcRNF135 functions as an E3 ubiquitin ligase to

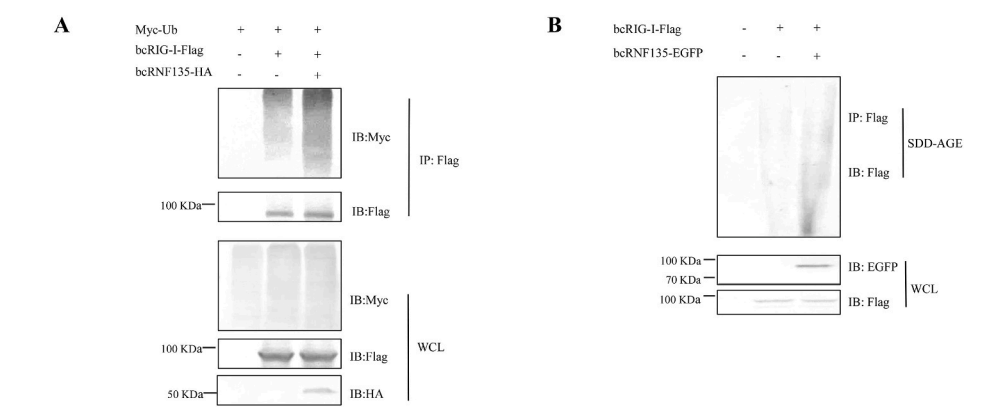


Fig. 8. bcRNF135 promoted the ubiquitination and oligomerization of bcRIG-I (A) HEK293T cells in 100 mm plates were co-transfected with Myc-Ub (5  $\mu$ g), bcRNF135-Flag (5  $\mu$ g) and/or bcRIG-I-HA (5  $\mu$ g), separately. The transfected cells were harvested for co-IP at 48 hpt. The total amount of plasmids was balanced with the empty vectors. (B) HEK293T cells in 100 mm plates were transfected with empty vector (15  $\mu$ g), empty vector (7.5  $\mu$ g) + bcRIG-I-Flag (7.5  $\mu$ g), or bcRIG-I-Flag (7.5  $\mu$ g) + bcRNF135-EGFP (7.5  $\mu$ g), respectively. At 48 hpt, cells were collected and applied for SDD-AGE.

promote the ubiquitination of bcRIG-I, which is a critical step for RIG-I activation. Furthermore, the SDD-AGE assay was employed to examine the effect of bcRNF135 on the oligomerization of bcRIG-I, a key process required for its full activation in antiviral signaling. The data in Fig. 8B demonstrated that cells expressing both bcRNF135 and bcRIG-I showed a marked increase in the formation of high-molecular-weight oligomers of bcRIG-I compared to cells expressing bcRIG-I alone. To conclude, the above results show that bcRNF135 promotes the ubiquitination and oligomerization of bcRIG-I, thereby potentiating its antiviral function.

#### 4. Discussion

Upon viral infection, RIG-I undergoes a conformational change that exposes its caspase activation and recruitment domains (CARDs), enabling the binding of viral RNA ligands [22]. This interaction triggers a series of downstream signaling events leading to the activation of interferon regulatory factors (IRFs) and nuclear factor kappa B (NF- $\kappa$ B), culminating in the transcription of type I interferons and proinflammatory cytokines [23]. In this study, we identified the RNF135 homolog in black carp (*Mylopharyngodon piceus*) and found that bcRNF135 acts as a positive regulator of bcRIG-I in the host's antiviral innate immune response.

To investigate the expression pattern of RNF135 in host cells, we measured the mRNA level changes of RNF135 in MPK and MPF cells treated with various stimuli. The results showed that after SVCV infection and poly (I:C) stimulation, the transcription level of RNF135 increased, indicating its involvement in the response to viral infection (Fig. 2). This result is consistent with the findings of Oshiumi and Lai [15,24]. In addition, knocking down bcRNF135 significantly weakened the antiviral ability of host cells, indicating that bcRNF135 plays a positive regulatory role in the host's antiviral innate immune responses. We further investigated the functional role of bcRNF135 on bcRIG-I. Interestingly, our data indicate that the transcription levels of IFN promoters and SVCV components remain comparable to controls when bcRNF135 is expressed alone (Figs. 4 and 5). This observation suggests that bcRNF135 may require the presence of bcRIG-I to exert its positive regulatory effect. Co-transfection experiments clearly demonstrated that bcRNF135 significantly enhances the transcriptional activation of IFN promoters only when bcRIG-I is present, highlighting a synergistic interaction between these two proteins. Furthermore, the interaction bcRNF135 and bcRIG-I was confirmed co-immunoprecipitation and immunofluorescence assays (Fig. 7). This synergy underscores the importance of bcRNF135 in the RIG-I signaling pathway, acting as a co-factor that amplifies RIG-I-mediated immune responses. Previous studies by Oshiumi and colleagues first reported

that RNF135 binds to the C-terminal regulatory domain (RD) of RIG-I and mediates the K63-linked polyubiquitination of RIG-I [16]. Similarly, zebrafish RNF135 (zbRNF135) has been shown to promote K63-linked ubiquitination of zbRIG-I [24]. In our study, we confirmed that bcRNF135 enhances the ubiquitination of bcRIG-I, consistent with these earlier findings, thereby supporting the conserved role of RNF135 across different species in regulating the RIG-I pathway.

In mammals, the oligomerization of RIG-I is a critical step in signal amplification and propagation [25]. The binding of viral RNA to one RIG-I molecule induces a conformational change, facilitating the oligomerization of adjacent RIG-I molecules and the formation of a higher-order complex [26]. This oligomeric structure serves as a platform for the recruitment and activation of downstream signaling molecules, amplifying the antiviral response [27]. Several factors have been reported to participate in RIG-I's oligomerization. For example, TRIM25 enhanced the k63-linked polyubiquitination of RIG-I and the ubiquitination promoted the oligomerization of RIG-I to initiate the signaling cascade [16,28,29]. Upon poly (I:C) stimulation, RIG-I formed oligomers and the co-expression with MARCH5 reduces the expression of RIG-I oligomers [30]. Moreover, histone deacetylase 6 (HDAC6) facilitated RIG-I's oligomerization and promoted antiviral immunity to restrict RNA virus infection [31]. ZAPS associated with RIG-I to enhance the oligomerization of RIG-I, which resulted in the robust activation of IRF3 and NF-κB [32]. However, the regulatory mechanism on the oligomerization of RIG-I in teleosts remains largely unknown. To address this gap, we utilized SDD-AGE in this study, a technique that allows the detection of protein oligomerization, to explore the regulatory role of bcRNF135 on bcRIG-I. Our results indicated that bcRNF135 promotes the oligomerization of bcRIG-I, which suggests that this process is crucial for enhancing the antiviral signaling mediated by bcRIG-I. These findings contribute to our understanding of RIG-I regulation in teleosts' innate immune responses. The identification and characterization of bcRNF135 highlight its role in enhancing the antiviral activities mediated by bcRIG-I, shedding light on the intricate mechanisms underlying the activation and oligomerization of RIG-I in teleosts' innate immunity.

In conclusion, our results provide evidence that bcRNF135 plays a positive role in the regulation of the RIG-I signaling pathway in teleost. bcRNF135 associates with bcRIG-I and enhances the ubiquitination and oligomerization of bcRIG-I, promoting antiviral signaling against SVCV. This study reveals the function of RNF135 in black carp and contributes to the broader understanding of innate immunity in teleosts.

#### CRediT authorship contribution statement

Chushan Dai: Investigation, Writing - original draft. Yujia Miao:

Investigation. Zhan'ao Li: Investigation. Yumian Liu: Visualization. Ji Liu: Visualization. Xiaoyu Liu: Software. Shasha Tan: Investigation. Hui Wu: Methodology. Jun Xiao: Writing – review & editing. Jun Zou: Formal analysis. Hao Feng: Supervision, Project administration, Writing – review & editing.

#### Acknowledgements

This work was supported by the National Natural Science Foundation of China (U21A20268, U22A20535, U23A20252, 31920103016), Hunan Provincial Science and Technology Department (2023JJ40435, 2023JJ10028, 2022JJ30383), the Earmarked Fund for Hunan Agriculture Research System (HARS-07), Hunan Provincial Education Department (23B0070), the Research and Development Platform of Fish Disease and Vaccine for Post-graduates in Hunan Province, College students research learning and innovative experiment project of Hunan province (S202410542007, S202410542082).

#### Appendix A. Supplementary data

Supplementary data to this article can be found online at https://doi.org/10.1016/j.fsi.2024.109987.

#### Data availability

Data will be made available on request.

#### References

- [1] J. Xiao, H. Zhong, H. Feng, Post-translational modifications and regulations of RLR signaling molecules in cytokines-mediated response in fish, Dev. Comp. Immunol. 141 (2023) 104631, https://doi.org/10.1016/j.dci.2023.104631.
- [2] S. Akira, S. Uematsu, O. Takeuchi, Pathogen recognition and innate immunity, Cell 124 (2006) 783–801, https://doi.org/10.1016/j.cell.2006.02.015.
- [3] K.M. Quicke, M.S. Diamond, M.S. Suthar, Negative regulators of the RIG-I-like receptor signaling pathway, Eur. J. Immunol. 47 (2017) 615–628, https://doi.org/ 10.1002/eji.201646484.
- [4] B. Huang, Z.X. Wang, C. Zhang, S.W. Zhai, Y.S. Han, W.S. Huang, P. Nie, Identification of a novel RIG-I isoform and its truncating variant in Japanese eel, Anguilla japonica, Fish Shellfish Immunol. 94 (2019) 373–380, https://doi.org/ 10.1016/j.fsi.2019.09.037.
- [5] D.C. Beachboard, S.M. Horner, Innate immune evasion strategies of DNA and RNA viruses, Curr. Opin. Microbiol. 32 (2016) 113–119, https://doi.org/10.1016/j. mib.2016.05.015.
- [6] Y.-M. Loo, M. Gale, Immune signaling by RIG-I-like receptors, Immunity 34 (2011) 680–692, https://doi.org/10.1016/j.immuni.2011.05.003.
- [7] A. Solstad, O. Hogaboam, A. Forero, E.A. Hemann, RIG-I-like receptor regulation of immune cell function and therapeutic implications, J. Immunol. 209 (2022) 845–854, https://doi.org/10.4049/jimmunol.2200395.
- [8] C.E. Berndsen, C. Wolberger, New insights into ubiquitin E3 ligase mechanism, Nat. Struct. Mol. Biol. 21 (2014) 301–307, https://doi.org/10.1038/nsmb.2780
- [9] M. Akutsu, I. Dikic, A. Bremm, Ubiquitin chain diversity at a glance, J. Cell Sci. 129 (2016) 875–880, https://doi.org/10.1242/jcs.183954.
- [10] N. Zheng, N. Shabek, Ubiquitin ligases: structure, function, and regulation, Annu. Rev. Biochem. 86 (2017) 129–157, https://doi.org/10.1146/annurev-biochem-060815-014922.
- [11] M.U. Gack, Y.C. Shin, C.-H. Joo, T. Urano, C. Liang, L. Sun, O. Takeuchi, S. Akira, Z. Chen, S. Inoue, J.U. Jung, TRIM25 RING-finger E3 ubiquitin ligase is essential for RIG-I-mediated antiviral activity, Nature 446 (2007) 916–920, https://doi.org/10.1038/nature05732.
- [12] L. Wang, W. Zhao, M. Zhang, P. Wang, K. Zhao, X. Zhao, S. Yang, C. Gao, USP4 positively regulates RIG-I-mediated antiviral response through deubiquitination and stabilization of RIG-I, J. Virol. 87 (2013) 4507–4515, https://doi.org/10.1128/JVI.00031-13.
- [13] C. Zhao, M. Jia, H. Song, Z. Yu, W. Wang, Q. Li, L. Zhang, W. Zhao, X. Cao, The E3 ubiquitin ligase TRIM40 attenuates antiviral immune responses by targeting MDA5

- and RIG-I, Cell Rep. 21 (2017) 1613–1623, https://doi.org/10.1016/j.celrep.2017.10.020.
- [14] Y. Jin, K. Jia, W. Zhang, Y. Xiang, P. Jia, W. Liu, M. Yi, Zebrafish TRIM25 promotes innate immune response to RGNNV infection by targeting 2CARD and RD regions of RIG-I for K63-linked ubiquitination, Front. Immunol. 10 (2019) 2805, https:// doi.org/10.3389/fimmu.2019.02805.
- [15] H. Oshiumi, M. Matsumoto, S. Hatakeyama, T. Seya, Riplet/RNF135, a RING finger protein, ubiquitinates RIG-I to promote interferon-β induction during the early phase of viral infection, J. Biol. Chem. 284 (2009) 807–817, https://doi.org/10.1074/jbc.M804259200.
- [16] H. Oshiumi, M. Miyashita, M. Matsumoto, T. Seya, A distinct role of riplet-mediated K63-linked polyubiquitination of the RIG-I repressor domain in human antiviral innate immune responses, PLoS Pathog. 9 (2013) e1003533, https://doi.org/10.1371/journal.ppat.1003533.
- [17] H. Oshiumi, M. Miyashita, N. Inoue, M. Okabe, M. Matsumoto, T. Seya, The ubiquitin ligase riplet is essential for RIG-I-dependent innate immune responses to RNA virus infection, Cell Host Microbe 8 (2010) 496–509, https://doi.org/ 10.1016/j.chom.2010.11.008.
- [18] J. Liu, C. Dai, L. Yin, X. Yang, J. Yan, M. Liu, H. Wu, J. Xiao, W. Kong, Z. Xu, H. Feng, STAT2 negatively regulates RIG-I in the antiviral innate immunity of black carp, Fish Shellfish Immunol. 148 (2024) 109510, https://doi.org/10.1016/j.fsi.2024.109510.
- [19] Y. Liu, J. Xiao, G. Qiao, Q. Wang, X. Yang, X. Xu, J. Li, J. Zhang, M. Chang, H. Feng, DDX19 inhibits RLR/IRF3 mediated type I interferon signaling of black carp Mylopharyngodon piceus by restricting IRF3 from entering nucleus, Aquaculture 553 (2022) 738087, https://doi.org/10.1016/j.aquaculture.2022.738087.
- [20] T.J. Hayman, A.C. Hsu, T.B. Kolesnik, L.F. Dagley, J. Willemsen, M.D. Tate, P. J. Baker, N.J. Kershaw, L. Kedzierski, A.I. Webb, P.A. Wark, K. Kedzierska, S. L. Masters, G.T. Belz, M. Binder, P.M. Hansbro, N.A. Nicola, S.E. Nicholson, RIPLET, and not TRIM25, is required for endogenous RIG-I-dependent antiviral responses, Immunol. Cell Biol. 97 (2019) 840–852, https://doi.org/10.1111/imcb.12284.
- [21] D. Gao, Y.-K. Yang, R.-P. Wang, X. Zhou, F.-C. Diao, M.-D. Li, Z.-H. Zhai, Z.-F. Jiang, D.-Y. Chen, REUL is a novel E3 ubiquitin ligase and stimulator of retinoic-acid-inducible gene-I, PLoS One 4 (2009) e5760, https://doi.org/10.1371/journal.pone.0005760.
- [22] J. Rehwinkel, M.U. Gack, RIG-I-like receptors: their regulation and roles in RNA sensing, Nat. Rev. Immunol. 20 (2020) 537–551, https://doi.org/10.1038/s41577-020-0288-3.
- [23] C. Yang, L. Liu, J. Liu, Z. Ye, H. Wu, P. Feng, H. Feng, Black carp IRF5 interacts with TBK1 to trigger cell death following viral infection, Dev. Comp. Immunol. 100 (2019) 103426, https://doi.org/10.1016/j.dci.2019.103426.
- [24] Y. Lai, M. Liang, L. Hu, Z. Zeng, H. Lin, G. Yi, M. Li, Z. Liu, RNF135 is a positive regulator of IFN expression and involved in RIG-I signaling pathway by targeting RIG-I, Fish Shellfish Immunol. 86 (2019) 474–479, https://doi.org/10.1016/j. fsi.2018.11.070.
- [25] E. Kowalinski, T. Lunardi, A.A. McCarthy, J. Louber, J. Brunel, B. Grigorov, D. Gerlier, S. Cusack, Structural basis for the activation of innate immune pattern-recognition receptor RIG-I by viral RNA, Cell 147 (2011) 423–435, https://doi. org/10.1016/j.cell.2011.09.039
- [26] C.M. Zerbe, D.J. Mouser, J.L. Cole, Oligomerization of RIG-I and MDA5 2CARD domains, Protein Sci. 29 (2020) 521–526, https://doi.org/10.1002/pro.3776.
- [27] B. Wu, S. Hur, How RIG-I like receptors activate MAVS, Current Opinion in Virology 12 (2015) 91–98, https://doi.org/10.1016/j.coviro.2015.04.004.
- [28] W. Zeng, L. Sun, X. Jiang, X. Chen, F. Hou, A. Adhikari, M. Xu, Z.J. Chen, Reconstitution of the RIG-I pathway reveals a signaling role of unanchored polyubiquitin chains in innate immunity, Cell 141 (2010) 315–330, https://doi. org/10.1016/j.cell.2010.03.029.
- [29] T. Saito, R. Hirai, Y.-M. Loo, D. Owen, C.L. Johnson, S.C. Sinha, S. Akira, T. Fujita, M. Gale, Regulation of innate antiviral defenses through a shared repressor domain in RIG-1 and LGP2, Proc. Natl. Acad. Sci. U.S.A. 104 (2007) 582–587, https://doi. org/10.1073/pnas.0606699104.
- [30] Y.-J. Park, N.T.K. Oanh, J. Heo, S.-G. Kim, H.-S. Lee, H. Lee, J.-H. Lee, H.C. Kang, W. Lim, Y.-S. Yoo, H. Cho, Dual targeting of RIG-I and MAVS by MARCH5 mitochondria ubiquitin ligase in innate immunity, Cell. Signal. 67 (2020) 109520, https://doi.org/10.1016/j.cellsig.2019.109520.
- [31] H.M. Liu, F. Jiang, Y.M. Loo, S. Hsu, T.-Y. Hsiang, J. Marcotrigiano, M. Gale, Regulation of retinoic acid inducible gene-1 (RIG-I) activation by the histone deacetylase 6, EBioMedicine 9 (2016) 195–206, https://doi.org/10.1016/j. ebiom.2016.06.015.
- [32] S. Hayakawa, S. Shiratori, H. Yamato, T. Kameyama, C. Kitatsuji, F. Kashigi, S. Goto, S. Kameoka, D. Fujikura, T. Yamada, T. Mizutani, M. Kazumata, M. Sato, J. Tanaka, M. Asaka, Y. Ohba, T. Miyazaki, M. Imamura, A. Takaoka, ZAPS is a potent stimulator of signaling mediated by the RNA helicase RIG-I during antiviral responses, Nat. Immunol. 12 (2011) 37-44, https://doi.org/10.1038/ni.1963.